25th ABCM International Congress of Mechanical Engineering
October 20-25, 2019, Uberlândia, MG, Brazil

COB-2019-1359
INFLUENCE OF FSW PROCESS PARAMETERS ON THE MAGNITUDE OF RESIDUAL STRESSES IN AA7075-T651 ALUMINUM ALLOY WELDED JOINTS

Jefferson Segundo de Lima
Theophilo Moura Maciel
Universidade Federal de Campina Grande, UFCG, R. Aprígio Veloso, 882 - Universitário, Campina Grande - PB - Brasil
jefferson_2seg@gmail.com; theophilo.maciel@ufcg.edu.br

Oclávio Coutinho dos Santos
Amós Freitas de Figueirêdo
Raphael Henrique Falcão de Melo
Instituto Federal de Educação, Ciências e Tecnologia, IFPB, R. José Antônio da Silva, 300 - Jardim Oásis, Cajazeiras - PB - Brasil
oklavyo@gmail.com; amos.figueiredo@gmail.com; raphael.melo@ifpb.edu.br

Abstract.
Aluminum alloys has excellent characteristics and mechanical properties. The 7xxx series of aluminum alloys, in particular, have a high mechanical resistance. However, the welding of thermally treatable aluminum alloys by conventional arc welding process results in an excessive degradation its mechanical resistance and inceasing its residual stress level. In this context, Frinction Stir Welding (FSW) process has received attention in recent years mainly because it does not reach the melting point of the material during the process. This work aims to analyze the influence of the parameter process in tesile strenght and residual stresses of AA7075 alloy welded joint by FSW process. For this purpose, tool rotational speed and welding speed were varied using the Design of Experiments method. They were obtained welded joints with low residual stresses, yield strength (YS) above 50% of the YS of the base metal and with ultimate tensile strength of up to 380 MPa. The results shows that a high tool rotational speed, around 1415 RPM, generates lower levels of residual stresses. With realization of design of experiment (DOE), it was found that the welding speed is the dominant parameter to determine the magnitude of longitudinal residual stresses of FSW joints.

Keywords: *Friction stir welding, aluminum alloys, residual stresses, aluminum 7xxx.*

1. INTRODUCTION

Among the various types of aluminum alloys, Al - Zn alloys (7xxx series) are the most used in aeronautical industry because offer an excellent relation between weight lower and high mechanical resistance (Cavaliere, 2013; Zaman, Noor, Khan, & Mukhopadhyay, 2017). However, welding of these kind of aluminum alloys by fusion conventional process, requires a number of precautions in order to avoid loss of mechanical properties due to the precipitate coalescing, formation of coarse structures of solidification, distortion and high residual stresses level among others defects related to solidification, (Lee, Lee, Yeon, & Jung, 2005; Maggiolini, Tovo, Susmel, James, & Hattingh, 2016; Yang et al., 2018). To overcome such difficulties imposed by traditionally welding process, application of friction welding process where the joining of parts occurs without fusion, have been used. in a more intense way (Capelari & Mazzaferro, 2009; Texier et al., 2018).

Developed and patented by The Welding Institute (TWI) in 1991, the Friction Stir Welding (FSW) process consists of an high mechanical strength rotating tool with a special profile, which is inserted into the material advancing continuously, generating heat and promoting a mechanical mixing of the metals involved, making a high quality welded joint without the need of filler metal (Padhy, Wu, & Gao, 2018). However, the FSW process has several variables which influence the welded joint performance such as tool rotational speed, tool geomety, welding speed, tool tilt angle, axial force and tool shoulder input. So, a prospective studies to achive the adequated welding parameter is necessary (Aval, 2015; Ji et al., 2015; Sutton, Reynolds, Wang, & Hubbard, 2002).

Residual stresses are accumulated in welded joints as a consequence of welding, and may reduce the mechanical strength of joints, such as fatigue life, as well as corrosion resistance. Residual stresses are the result of non-homogeneous microstructural transformations that imply volumetric changes due to the intense and localized heat input

of the arc welding process, resulting in different behavior in each region of the joint with different temperatures, different cooling rates and different microstructures (Ji et al., 2015). This is not verified with the same intensity in solid state welding processes, such as FSW (Oliveira et al., 2018).

The rapid cooling during welding of aluminum alloys, due to high thermal conductivity, associated with the high coefficient of thermal expansion and low modulus of elasticity, and, high yield point, introduces high magnitude of residual stresses in welded joints of that material.

Due the excellent results obtained in technological and industrial development, statistical tools are increasingly used to obtain an optimization of industrial processes, and when combined with Desing Of Experimental (DOE), they become indispensable tools in establishment of statistical control of processes. The DOE represents a set of tests established with criteria scientific and statistical, in order to determine the influence of several variables on results of a system or process (Rodrigues & Iemma, 2014).

In this context, this work aims to evaluate the influence of FSW process variables, applying statistical tools with DOE, in the magnitude of residual stresses in AA7075-T651 aluminum alloy welded joints, with high confidence level.

2. METHODOLOGY

In this work aluminum plates of 7075-T651 alloy with 5 mm of thickness were used. The nominal chemical composition of the plates, according to the manufacturer, is presented in Tab. 1.

Table 1. AA7075-T651 alloy nominal chemical composition (%).

Zn	Mg	Cu	Cr	Al
5.6	2.5	1.6	0.23	Balanço

The mechanical properties of the base metal (BM) obtained in the uniaxial tensile test, is presented in Tab. 2.

Table 2. Mechanical properties of the base metal.

Material	Yield strength (MPa)	Ultimate tensile strength (MPa)	Strain (%)
7075-T651	500	575	11.7

The tool used in FSW process has a cylindrical straight threaded pin geometry. The FSW tool and its dimensions are shown in Fig. 1. It was machined from an carbon steel ABNT 1020 plate and afteward subjected to cementation at 925 °C for 4 hours, followed by quenching in stirred water, in order to increase the hardness and wear resistance of the tool pin and shoulder.

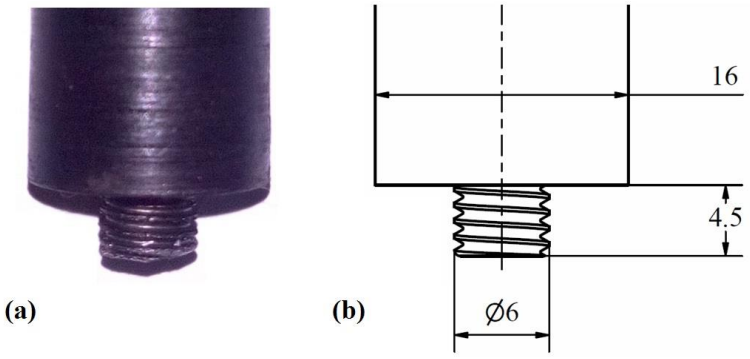

Figure 1. FSW tool: (a) manufactured and (b) project dimension (in ‘mm’).

The FSW welded joints were made using a Diplomat FU-300 automatic universal milling machine, with adjust of the transverse speed, tool inclination and rotation. The tool tilt angle was maintained at 3 ° throughout the process. The dimensions of the welded joint sample was 5x50x120 mm.

The chosen level of the process parameters with their units and notations are presented in Tab. 3. In order to ascertain the influence of the parameters 8 welded joints were done, according to design of experiment 2^2 with replica.

Table 3. Summary for variables.

FACTORS	NOTATION	LOW - VALUE	HIGH - VALUE
Tool rotational speed (RPM)	A	410	1415
Welding speed (mm/s)	B	48	118

The combination of parameters/factors for fabrication of welded joints can be observed from table 4.

Table 4. Combination parameters – welded joints.

NOTATION		WELDED JOINT
A (RPM)	B (mm/s)	
410	48	1
1415	48	2
410	118	3
1415	118	4

In order to determine the tensile strength, tensile tests were performed using a MTS universal test machine, model 810. The dimensions of the test specimens for tensile testing are shown in Fig. 2.

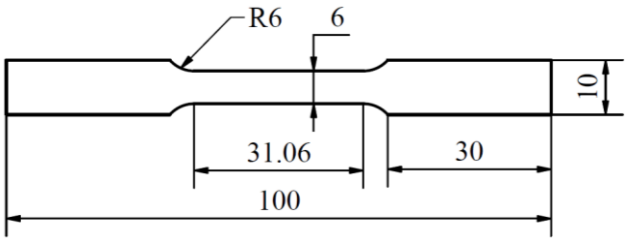

Figure 2. Dimension of flat tensile specimens (in 'mm').

Finally, in order to determine the magnitude of the residual stresses in the welded joints, a variation of the semi-destructive technique of the blind hole was used, as developed by Siqueira Filho et al (2013). The method consists of an coordinate measuring machine which determine the variation of the predetermined coordinates to the center of a hole after it has been made. It is expected that variation of the coordinates occurs as a function of the relaxation of residual stresses welding. Considering the Eqs. (1) e (2):

$$\sigma_x = \frac{E}{1-\nu^2}\left(\varepsilon_x + \nu\varepsilon_y\right) \tag{1}$$

$$\sigma_y = \frac{E}{1-\nu^2}\left(\varepsilon_y + \nu\varepsilon_x\right) \tag{2}$$

where: σ_x is the Longitudinal residual stress - direction of the weld [Pa]; σ_y is the Transverse residual stress - direction normal to the weld line [Pa]; E Elasticity module; ν is the Poisson's ratio; ε_x is the Deformation in the direction of welding; ε_y is the Deformation in the direction of Normal strain at the weld line.

Considering the reference coordinates equivalent to the coordinates of the central points of the holes, produced in machining center, the ε_y, at each point, is given by the relation between reference coordinate and the coordinate determined in Y, obtained by coordinate measuring machine, similarly, the ε_x is given by the relationships between the coordinates references and determined in X. Considering the Eqs. (3) e (4):

$$\varepsilon_y = \frac{y_f - y_i}{y_i} \tag{3}$$

$$\varepsilon_x = \frac{x_f - x_i}{x_i} \tag{4}$$

Where: y_i is the value of Y in the center coordinate of the hole;; y_f is the value of Y at the determined coordinate of the center of the hole; x_i is the value of Y at the hole center reference coordinate; x_f is the value of X at the determined coordinate of the hole center.

The reference coordinates were determined in a CNC program, in FANUC code, and the holes were made using a Romi D-600 machining center. Distribution of small holes is observed in Fig. 3. The coordinates after drilling were determined using a TESAMICROHITE 3D coordinate measuring machine, with a resolution of 0.1 μm.

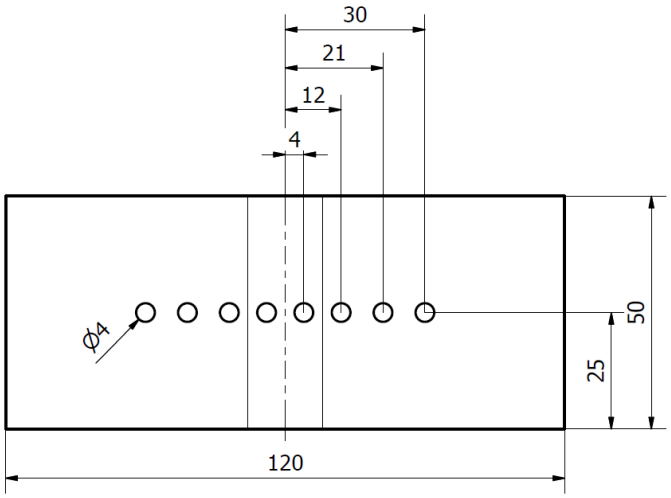

Figure 3. Distribution of small holes for measuring residual stress (dimensions in mm).

In order to ensure good reliability, five coordinate determinations were made for the center point of each hole in each welded joint, using the mean values to obtain the magnitude of residual stresses.

3. RESULTS

In the Fig. 4 it's possible to observe the FSW weld bead in one of the welded joints, defects associated with voids and irregularities were not visually observed. There is an excess of deburring on the retreating side of the welded joint due to compressive plastic deformation of the material surrounding the tool, especially on the retreating side of the weld.

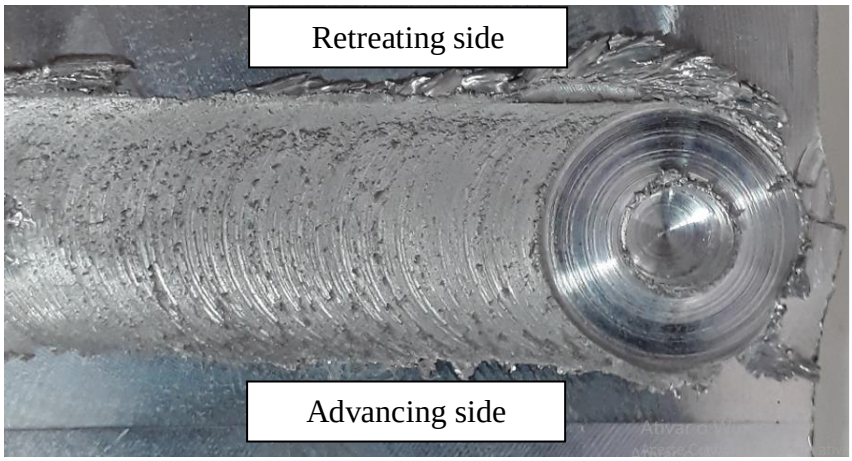

Figure 4. Weld FSW aluminum AA7075-T651.

3.1 Tensile strength analysis

Watching Fig. 5, the stress-strain curves generated during the tensile test of welded joints, it can be verified that the rotation had the main influence on the tensile strength of the material.

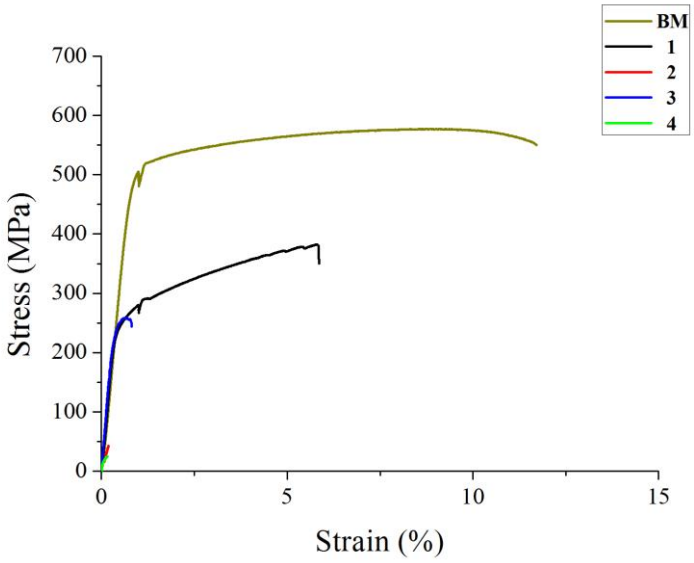

Figure 5. Stress-strain behavior for welded joints.

In Fig. 5, the yield strength (YS), ultimate tensile strength (UTS) and deformation to base metal fracture are higher than those of welded joints, results already expected. Due to the growth and elongation of the grains in the thermally affected zone (HAZ) as a result of the heat of friction generated by the relative speed between the rotary tool and the substrate (Sarsilmaz, 2018).

It was also observed that the welded joints 1 and 3, obtained with lower rotation speed, 410 RPM, presented better stress-strain behavior, reaching higher values of YS, UTS and strain. While welded joints 2 and 4, with higher rotational speed of 1415 RPM, presented lower performance, occurring fragile fracture without plastic deformation. Consequence of higher heat input generated during the process.

Increased rotational speed led to lower tensile strength due to higher heat input leading to higher temperatures in the heat affected zones, increasing the effects of grain growth and precipitate dissolution.

The tool rotational speed of 410 RPM and welding speed of 48 mm/s guaranteed a UTS of 380 MPa to joint 1 for this work, performance conventionally superior to arc welded joints. according to literature (Olabode, Kah, Hiltunen, & Martikainen, 2016; Sivashanmugam, Jothi Shanmugam, Kumar, & Sathishkumar, 2010; Temmar, Hadji, & Sahraoui, 2011).

3.2 Residual stress analysis

So far, graphs of residual stress levels of FSW welded joints have been obtained by varying the parameters of tool rotation speed and welding speed presented in Fig. 6.

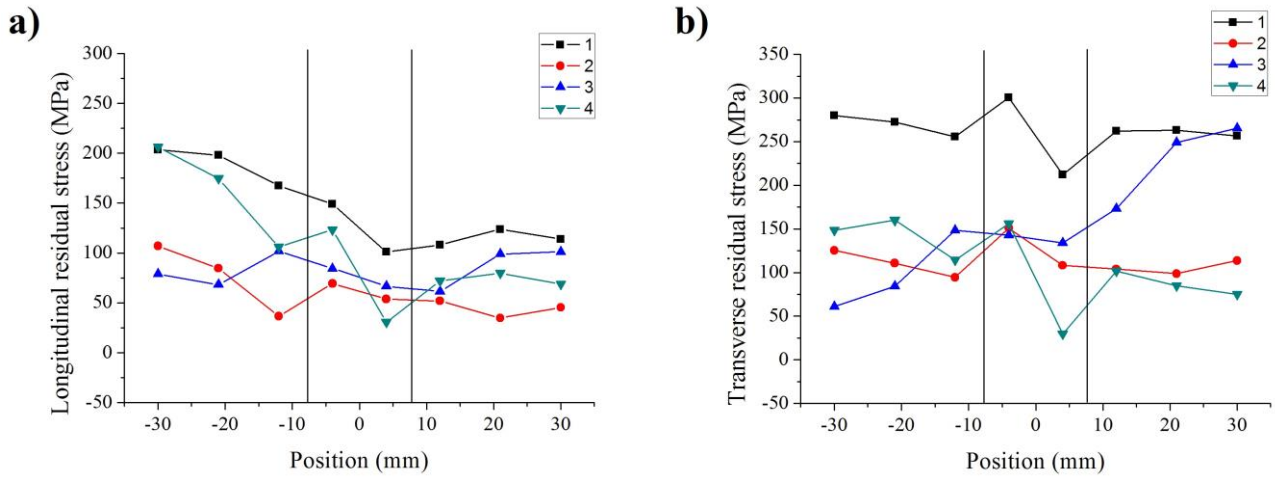

Figure 6. Distribution longitudinal and transverse residual stress.

Analyzing the longitudinal residual stresses, in Fig. 6, it is observed only the existence of tensile tensions throughout the welded joint region, regardless of the parameter used, presenting higher values in the retreating side of the welded joint, similar to that observed by Oliveira, *et al* (2018). The presence of the tensile residual stress was attributed to the compressive plastic deformation of the material surrounding the tool, mainly in the retreating side. It was found that welded joint 1 obtained higher levels of residual stresses.

The transverse residual stress also obtained only tensile stresses. In addition, the transverse residual stress have a maximum magnitude of the order of 300 MPa and a minimum of 30 MPa. It is noteworthy that all welded joints had residual stresses of magnitude lower than the YS in BM of 500 MPa.

Following the analysis regarding the transverse residual stresses, it is noted that for the welded joints 1, 2 and 4 the point of greatest tensile residual stress occurred 8 mm apart in relation to the center of the weld, on the retreating side, whereas for at weld joint 3 this point occurred on the feed side, 30 mm from the weld center line. The combination of fabrication parameters of welded joint 3, provides more difficult joining and lower heat input. It can be inferred that the decrease in temperature in this welded joint made it difficult to perform welding, requiring greater force in the tool advance, and that during cooling, due to the material being less heated, cooling was faster, and consequently the residual stress increased, generating a more irregular profile of tensions. Analyzing the mixing region, approximately the range - 8 to 8, corresponding to the shoulder diameter of the tool, it is observed that there is practically no difference in the behavior of residual stress profiles between welded joints, showing a decrease in the value of the weld joints. indentation side to the advance side.

Welded joint 2, with tool rotation speed of 1415 RPM and welding speed of 48 mm/s, in relation to the generated residual stresses, obtained lower levels of tensile longitudinal and transverse residual stresses, which is directly related to the chosen parameters for the realization of the weld. Since increased tool rotation speed and lower welding speed tends to facilitate the mechanical work of deformation in the FSW due to the greater softening of the material, ensuring almost completely homogeneous plasticization and greater flow ability of the metal mixture in the Stir Zone (SZ) (Delijaicov, Silva, Resende, & Batalha, 2018), not contributing to the increase of residual stress levels, especially the compressive ones. The opposite can be seen in welded joints 1 and 3, with low tool rotation speeds of 410 RPM, making material flow difficult due to the lower heat input, thus generating higher residual stress levels.

In the case of brazed joint 4, even with a higher rotational speed of 1415 RPM, it presented higher levels of residual longitudinal tensile stress than brazed joint 2, as a result of the higher welding speed of 118 mm/s, nullifying the one made of greater mixing characteristic of higher tool rotation speeds, due to the shorter tool rotation time in the same place making it difficult to heat the region and generating greater efforts for the tool movement, thus reducing the plasticization homogeneity (Delijaicov et al., 2018).

3.3 Experimental analysis

From this study, we expect an empirical relationship capable of effectively predict the magnitude of residual stresses of FSW joints at the 95% per cent confidence level. In addition, we will try to evaluate the contour curves and the graph of the response surface to obtain the welding conditions in which the lowest levels of residual stress are configured.

Table 5 shows the results of experimental measurements according to the with replica design. The independent variables of the experiment are tool rotational speed (A) and welding speed (B). The dependent variables are longitudinal residual stress and transverse residual stress, referring to the average of the levels residual stress in range of position -10 and 10, approximately the limit of the thermally affected zone.

Table 5. Design of experiment 2^2 with replica.

Replicate	FACTOR		REDISUAL STRESS	
	A	B	Longitudinal [MPa]	Transverse [MPa]
1	-1	-1	103	153
1	1	-1	107	188
1	-1	1	63	121
1	1	1	73	160
2	-1	-1	106	162
2	1	-1	97	191
2	-1	1	59	116
2	1	1	71	157

Using the software Statistica, the analysis of variance (ANOVA) was performed in order to study the influence of independent variables, such as rotation, feed and inclination angle of the tool, on the dependent variables chosen. For all variables we used the significance p=0,05.

An $R^2 = 0.9777$ and an adjusted $R^2 = 0.96098$ were obtained, which means that there is an approximately 96% adherence between the experimentally obtained values and the regression values. In the Pareto diagram of Fig. 7, it is possible to see that the parameter that most influenced the longitudinal residual stress variable is welding speed (B).

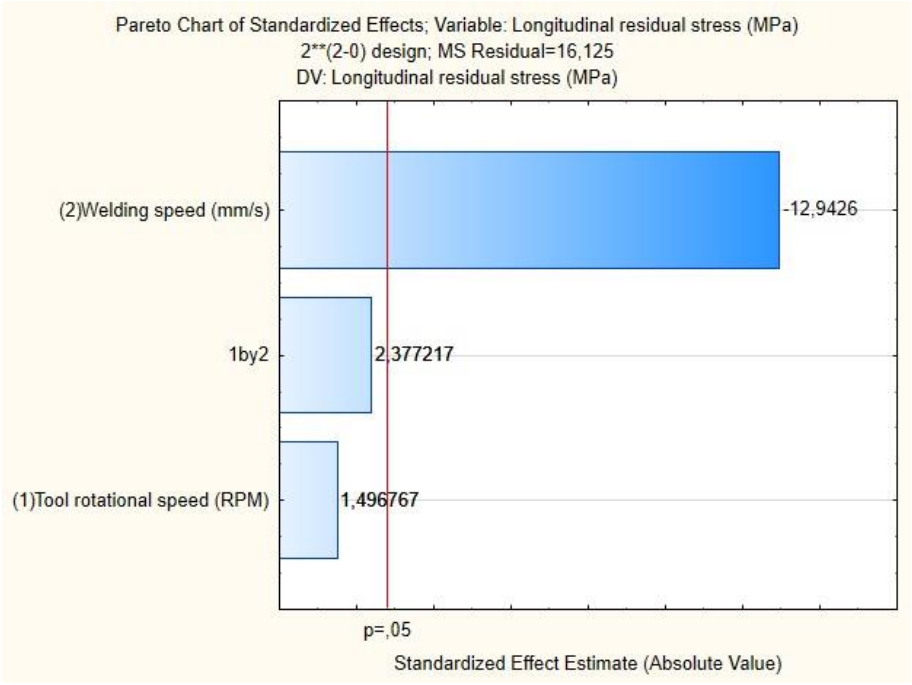

Figure 7. Pareto diagram of the longitudinal dependent variable residual stress.

As determined by experimental analysis, pareto diagram in Fig. 7, and according to Lombard, et al (2008), welding velocity is the dominant parameter for determining longitudinal residual stress peaks, since determines heat input per unit length of weld. Establishing the thermal cycle in terms of heating and cooling rate (Carlone & Palazzo, 2013) noted that increasing welding speed causes a more severe residual stress condition. Since it reduces the time available for heat diffusion away from the weld centerline, inducing higher temperature gradients and higher cooling stresses.

The Fig. 8 presents the influence of variables A and B on the longitudinal dependent variable residual stress.

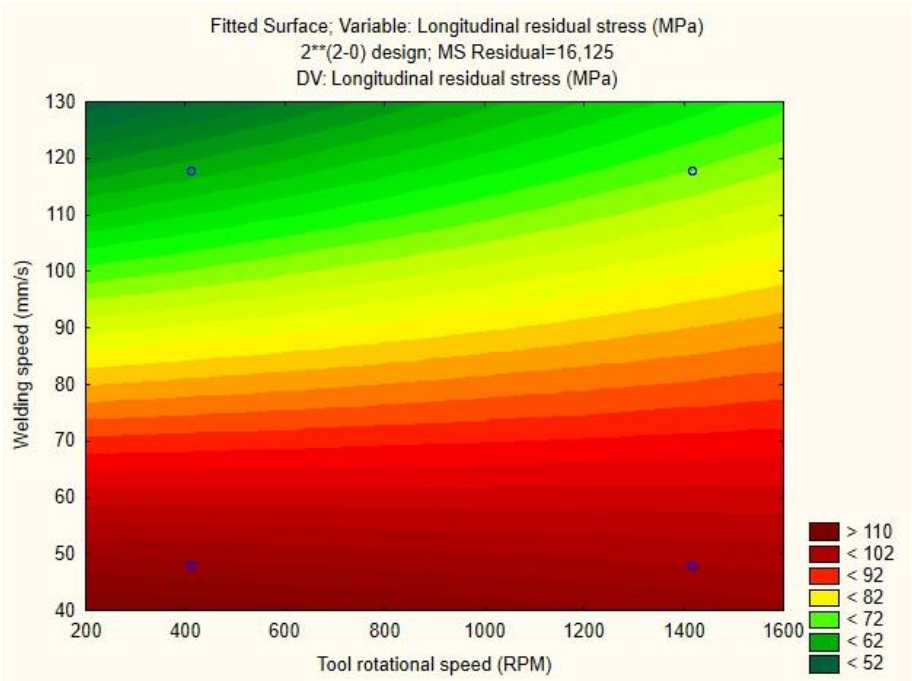

Figure 8. Surface graph of the influence of variables A and B on variable longitudinal residual stress.

An $R^2 = 0.98793$ and an adjusted $R^2 = 0.97887$ were obtained, which means that there is an approximately 97% adherence between the experimentally obtained values and the regression values. In the Pareto diagram of Fig. 9 it is possible to see that both parameters A and B significantly influenced the dependent variable transverse residual stress.

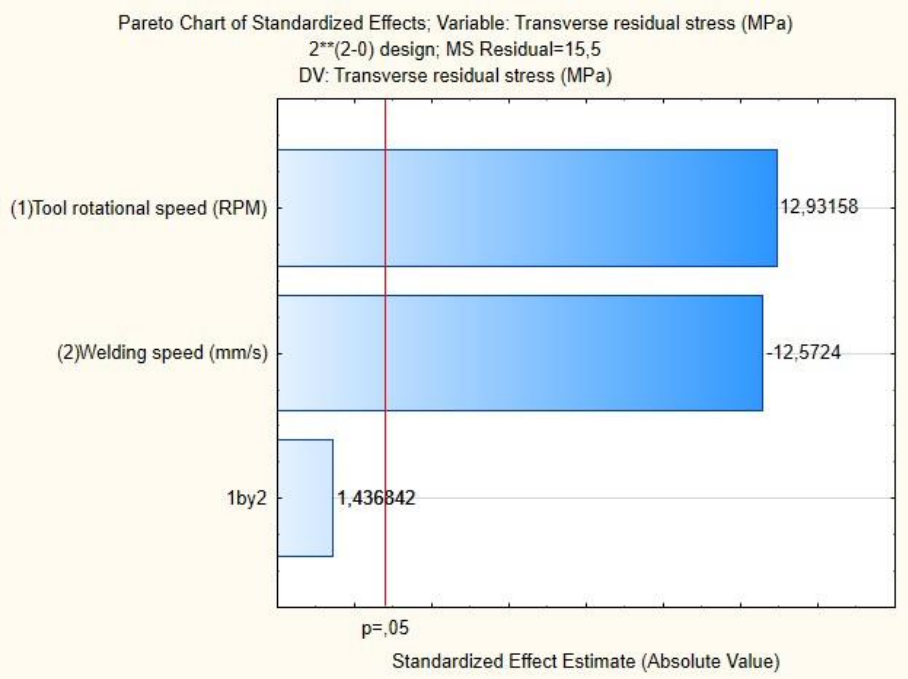

Figure 9. Pareto diagram of the dependent variable transverse residual stress.

The Fig. 10 shows the influence of variables A and B on the dependent variable transverse residual stress.

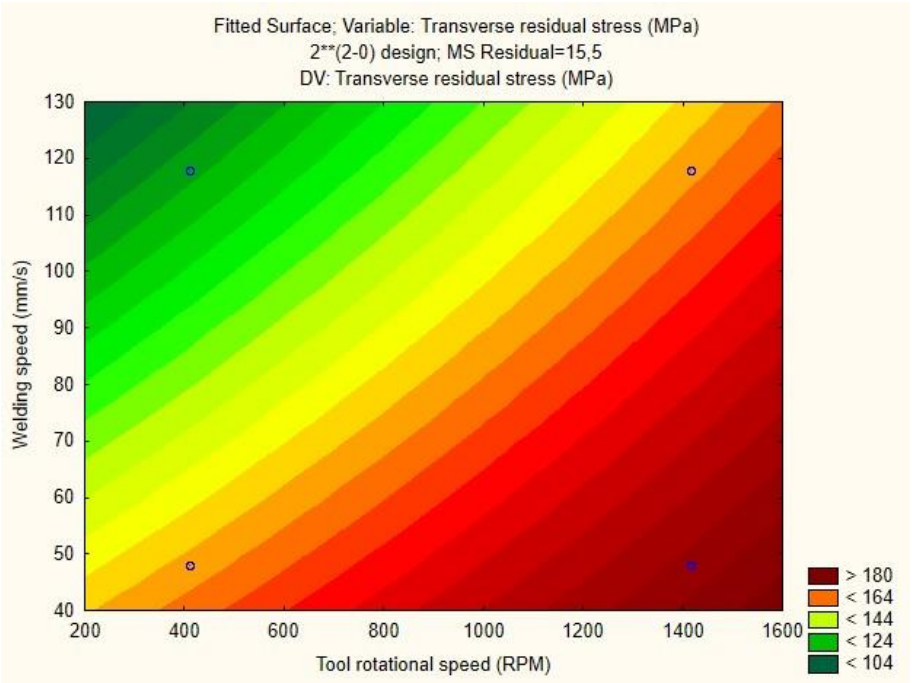

Figure 10. Surface graph of the influence of variables A and B on variable transverse residual stress.

Analyzing the Fig. 9 and Fig.10, both variables A and B present influence the transverse residual stress, being A inversely proportional to the high levels of residual stress, already B proportional directional. That is, lower values of welding speed and high values of tool rotational speed causes high levels of transverse residual stress.

4. CONCLUSIONS

Parameters of lower tool rotation speed of 410 RPM, coupled with lower welding speed of 48 mm/s, produced the highest stress-strain joint with an YS over 50% MB and an UTS up to 380 MPa without defects.

Regarding the residual stress profiles, it was found by experimental analysis that the welding speed is the dominant parameter to determine the longitudinal residual stress levels.

The interaction of the highest tool rotation speed of 1415 RPM and low welding speed of 48 mm/s did not contribute to the increase of residual stress levels in the welded joint. Generating profile with lower values of tractive residual stress.

5. ACKNOWLEDGEMENTS

The authors thank the PRPIPG of the *Instituto Federal de Educação, Ciência e Tecnologia da Paraíba* for the investment and scholarship, by means of the INTERCONECTA 2019. And the grant 285/18, Paraíba State Research Foundation (FAPESQ), by the grant of scholarship.

6. REFERENCES

Aval, H. J. (2015). Microstructure and residual stress distributions in friction stir welding of dissimilar aluminium alloys. *Materials & Design*, *87*, 405–413.

Capelari, T. V., & Mazzaferro, J. A. E. (2009). Avaliação da geometria de ferramenta e parâmetros do processo FSW na soldagem da liga de alumínio AA 5052. *Soldagem e Inspecao*, *14*(3), 215–227. https://doi.org/10.1590/S0104-92242009000300005

Carlone, P., & Palazzo, G. S. (2013). Influence of Process Parameters on Microstructure and Mechanical Properties in AA2024-T3 Friction Stir Welding. *Metallography, Microstructure, and Analysis*, *2*(4), 213–222. https://doi.org/10.1007/s13632-013-0078-4

Cavaliere, P. (2013). Friction stir welding of Al alloys: analysis of processing parameters affecting mechanical behavior. *Procedia CIRP*, *11*, 139–144.

Delijaicov, S., Silva, P. A. de O., Resende, H. B., & Batalha, M. H. F. (2018). Effect of Weld Parameters on Residual Stress, Hardness and Microstructure of Dissimilar AA2024-T3 and AA7475-T761 Friction Stir Welded Joints. *Materials Research*, *21*(6). https://doi.org/10.1590/1980-5373-mr-2018-0108

Ji, P., Yang, Z., Zhang, J., Zheng, L., Ji, V., & Klosek, V. (2015). Residual stress distribution and microstructure in the friction stir weld of 7075 aluminum alloy. *Journal of Materials Science*, *50*(22), 7262–7270. https://doi.org/10.1007/s10853-015-9280-x

Lee, C. Y., Lee, W. B., Yeon, Y. M., & Jung, S. B. (2005). The Joint Characteristics of Friction Stir Welded Mg-Zn-Y Alloy. *Materials Science Forum*, *475–479*, 555–558. https://doi.org/10.4028/www.scientific.net/MSF.475-479.555

Lombard, H., Hattingh, D. G., Steuwer, A., & James, M. N. (2008). Optimising FSW process parameters to minimise defects and maximise fatigue life in 5083-H321 aluminium alloy. *Engineering Fracture Mechanics*, *75*(3–4), 341–354. https://doi.org/10.1016/j.engfracmech.2007.01.026

Maggiolini, E., Tovo, R., Susmel, L., James, M. N., & Hattingh, D. G. (2016). Crack path and fracture analysis in FSW of small diameter 6082-T6 aluminium tubes under tension–torsion loading. *International Journal of Fatigue*, *92*, 478–487. https://doi.org/10.1016/j.ijfatigue.2016.02.043

Olabode, M., Kah, P., Hiltunen, E., & Martikainen, J. (2016). Effect of Al2O3 film on the mechanical properties of a welded high-strength (AW 7020) aluminium alloy. *Proceedings of the Institution of Mechanical Engineers, Part B: Journal of Engineering Manufacture*, *230*(11), 2092–2101.

Oliveira, E. B. S., Lima, J. S., Colaço, D. B., Ribeiro, M. A., Maciel, T. M., & Melo, R. H. F. (2018). Influência da geometria do pino da ferramenta de soldagem nas propriedades mecânicas e tensões residuais de juntas soldadas de ligas de alumínio 5052-O pelo processo FSW, *37*, 69–78. https://doi.org/10.17563/rbav.v37i2.1094

Padhy, G. K., Wu, C. S., & Gao, S. (2018). Friction stir based welding and processing technologies - processes, parameters, microstructures and applications: A review. *Journal of Materials Science and Technology*, *34*(1), 1–38. https://doi.org/10.1016/j.jmst.2017.11.029

Rodrigues, M. I., & Iemma, A. F. (2014). *Experimental Design and Process Optimization* (1st ed.). CRC Press.

Sarsilmaz, F. (2018). Relationship between micro-structure and mechanical properties of dissimilar aluminum alloy plates by friction stir welding. *Thermal Science*, *22*, S55–S66. https://doi.org/10.2298/TSCI170825271S

Siqueira Filho, A. V., Rolim, T. L., Yadava, Y. P., Cardoso, F. I. B., Maciel, T. M., & Ferreira, R. A. S. F. (2013). Development of Methodology for Measurements of Residual Stresses in Welded Joint Based on Displacement of Points in a Coordinated Table, *16*(2), 322–326. https://doi.org/10.1590/S1516-14392013005000001

Sivashanmugam, M., Jothi Shanmugam, C., Kumar, T., & Sathishkumar, M. (2010). Investigation of microstructure and mechanical properties of GTAW and GMAW joints on AA7075 aluminum alloy. *Proceedings of the International Conference on Frontiers in Automobile and Mechanical Engineering - 2010, FAME-2010*, *3*(2), 241–246. https://doi.org/10.1109/FAME.2010.5714843

Sutton, M. A., Reynolds, A. P., Wang, D., & Hubbard, C. R. (2002). A Study of Residual Stresses and Microstructure in 2024-T3 Aluminum Friction Stir Butt Welds, *124*(April). https://doi.org/10.1115/1.1429639

Temmar, M., Hadji, M., & Sahraoui, T. (2011). Effect of post-weld aging treatment on mechanical properties of Tungsten Inert Gas welded low thickness 7075 aluminium alloy joints. *Materials and Design*, *32*(6), 3532–3536. https://doi.org/10.1016/j.matdes.2011.02.011

Texier, D., Atmani, F., Bocher, P., Nadeau, F., Chen, J., Zedan, Y., … Demers, V. (2018). Fatigue performances of FSW and GMAW aluminum alloys welded joints: Competition between microstructural and structural-contact-fretting crack initiation. *International Journal of Fatigue*, *116*(June), 220–233. https://doi.org/10.1016/j.ijfatigue.2018.06.020

Yang, C., Ni, D. R., Xue, P., Xiao, B. L., Wang, W., Wang, K. S., & Ma, Z. Y. (2018). A comparative research on bobbin tool and conventional friction stir welding of Al-Mg-Si alloy plates. *Materials Characterization*, *145*(June), 20–28. https://doi.org/10.1016/j.matchar.2018.08.027

Zaman, N., Noor, A., Khan, Z. A., & Mukhopadhyay, A. K. (2017). Mechanical and microstructural behavior of friction stir welded similar and dissimilar sheets of AA2219 and AA7475 aluminium alloys. *Journal of Alloys and Compounds*, *695*, 2902–2908. https://doi.org/10.1016/j.jallcom.2016.11.389

7. RESPONSIBILITY NOTICE

The authors are the only responsible for the printed material included in this paper.